

## Preclinical report

# Ursolic acid triggers calcium-dependent apoptosis in human Daudi cells

F Lauthier,<sup>1</sup> L Taillet,<sup>1</sup> P Trouillas,<sup>2</sup> C Delage<sup>1</sup> and A Simon<sup>1</sup>

<sup>1</sup>Laboratoire de Chimie Physique et Minérale and <sup>2</sup>Laboratoire de Biophysique, Faculté de Pharmacie, 2 rue du Docteur Marcland, 87025 Limoges, France.

Ursolic acid (UA) is a pentacyclic triterpenoid compound which occurs naturally in a large variety of vegetarian foods, medicinal herbs and plants. In the present study, ursolic acid was found to decrease cell viability in human lymphoma Daudi cells in a dose-dependent manner. UA also induced morphological changes in cells as well as loss of membrane asymmetry, DNA fragmentation and nuclei condensation, indicating that the mechanism by which UA induced cell death was through apoptosis. Treatment with UA increased intracellular  $\text{Ca}^{2+}$  levels. Use of  $\text{Ca}^{2+}$  channel inhibitors like verapamil blocked this  $\text{Ca}^{2+}$  influx and also the triggering of apoptosis. We hypothesized that the binding of UA to glucocorticoid receptors and the  $\text{Ca}^{2+}$  currents induced constituted the first steps of apoptosis. [© 2000 Lippincott Williams & Wilkins.]

**Key words:** Apoptosis, calcium, Daudi cells, ursolic acid.

## Introduction

The search for new more effective and less toxic chemopreventive and antitumor agents has kindled great interest in phytochemicals. Ursolic acid (UA), a pentacyclic triterpene acid which is widely distributed in plants, but also in the waxlike coating of apples and other fruits,<sup>1,2</sup> is one such compound.

UA is known to have a pleiotropic biological activity profile.<sup>3</sup> UA has been reported to produce antitumor activities, including inhibition of tumor promotion<sup>4,5</sup> and inhibition of skin tumorigenesis.<sup>6</sup> It also induces tumor cell differentiation in F9 teratocarcinoma cells.<sup>7</sup> In addition, studies performed in our laboratory demonstrated that UA reduces the *in vitro* growth of a large list of cancer cell lines like human leukemic HL60 cells, human breast MCF7 cells and mouse

melanoma B16 cells.<sup>8–10</sup> In 1997, Baek *et al.* demonstrated that UA can cause, by as yet undefined mechanisms, apoptotic cell death on HL60 cells.<sup>11</sup>

Apoptosis is a physiological 'suicide process' by which cell number can be regulated without disruption of the overall tissue function. This phenomenon is characterized by morphological changes like chromatic condensation and formation of apoptotic bodies but also by loss of plasma membrane asymmetry and fragmentation of the nuclei.<sup>12</sup> Many studies focus on the fact that  $\text{Ca}^{2+}$  flux and their interaction with endonucleases could play a critical role in this process.<sup>13</sup>

Many of the chemotherapeutic agents presently used in cancer therapy such as cisplatin or camptothecin induce apoptosis.<sup>14,15</sup> According to gain knowledge concerning the anticancer properties of natural molecules commonly present in human feeding, we investigated the effect of UA on human lymphoma Daudi cell growth. Different techniques were used to identify and enumerate the part of cell death induced by apoptosis after UA treatment. The morphological and also the molecular aspects were investigated, and special attention was paid to intracellular calcium signals, which play a key role in molecular events of apoptosis.

## Materials and methods

### Cell culture

The Daudi cell line (Burkitt's human B cells) was maintained in RPMI 1640 medium supplemented with 10% heat-inactivated fetal calf serum, penicillin (100 U/ml) and streptomycin (100 mg/ml) at 37°C in a humidified atmosphere containing 5%  $\text{CO}_2$  (all products were purchased from Gibco, Grand Island, NY). Cells were split in a 3:100 ratio every 3 days and maintained in 75  $\text{cm}^2$  culture flasks. During experiments, Daudi cells were cultured and treated in 25  $\text{cm}^2$  culture flasks or in culture plates (Nunc, Roskilde, Denmark).

Correspondence to A Simon, Laboratoire de Chimie Physique et Minérale, Faculté de Pharmacie, 2 rue du Docteur Marcland, 87025 Limoges, France.  
Tel: (+33) 555 435 889; Fax: (+33) 555 435 911;  
E-mail: simon@unilim.fr

## UA treatment

UA was purchased from Sigma (St Louis, MO). A stock solution ( $10^{-2}$  M) was prepared in sterilized ethanol and stored at 4°C. Daudi cells were treated with different concentrations of UA (10–18  $\mu$ M). Controls were done with the same final ethanol concentration in the medium than in samples.

## Cell viability test (MTT staining)

In cell viability experiments, cells were plated in a concentration of  $10^4$  cells/well in 96-well flat-bottomed culture plates. At the end of an incubation period of 24 h in the presence of UA, cell viability was determined by the MTT staining method as described by Mosman.<sup>16</sup> This test is based on the selective ability of living cells to reduce the yellow soluble salt MTT (Sigma) to a purple-blue insoluble formazan precipitate. The amount of formazan metabolite formed was determined by an absorbance measure at 550 nm.

## Cytotoxicity evaluation by lactate dehydrogenase (LDH) release

The LDH assay is a colorimetric method to evaluate membrane integrity as a function of the amount of cytoplasmic LDH released in the medium. The experiments were composed of a control group (untreated cells) to determine the spontaneous release of LDH, a positive control (cells treated with 1% Triton X-100) to determine the maximum release of LDH and an experimental group (cells treated with UA or camptothecin). The detection procedures were in accordance with the Cytotoxicity Detection Kit instructions (Boehringer Mannheim, Mannheim, Germany). Briefly, at different times of treatment, samples supernatants were collected by centrifugation, transferred to a 96-well microtiter plate (Nunc), the reaction mixture was added to each well and incubated up to 20 min in the dark, at room temperature. The absorbance was measured at 490 nm using an ELISA plate reader (Muliskan Plus, Labsystems, Finland). The resulting values were substituted in the following equation :

$$\text{Cytotoxicity (\%)} = \frac{\text{experimental value} - \text{control value}}{\text{positive control value} - \text{control value}} \times 100$$

## Annexin V staining and flow cytometry

In the early stages of apoptosis, the plasma membrane loses its asymmetry and at this moment phosphatidylserine (PS) residues are exposed at the outer plasma membrane leaflet. Annexin V specifically binds to PS in

the presence of calcium. Daudi cells were treated with UA during 8 h, collected by centrifugation and stained by annexin V-fluorescein isothiocyanate (FITC), using the annexin V FLUOS kit (Boehringer Mannheim) according to the instructions of the manufacturer. Analysis of green (annexin V) and red [propidium iodide (PI) uptake] fluorescence was measured by FACS Vantage flow cytometer (Becton Dickinson, Mountain View, CA) using, respectively, a 530 (30) nm band pass filter and 600 nm long pass filter. At least  $10^4$  cells were collected and stored for each sample. Events were gated on FSC versus SSC in such a way that degraded DNA and cell debris were excluded.

## DNA isolation and electrophoresis

Cells ( $5 \times 10^5$ ) were incubated with UA (14–18  $\mu$ M) or camptothecin (0.1  $\mu$ M) in 25 cm<sup>2</sup> culture flasks. Daudi cells ( $10^6$ /assay) were collected after 24 h of treatment by centrifugation and lysed in a buffer containing 50 mM NaCl, 10 mM Tris (pH 7.6), 0.2% SDS, 0.02% proteinase K and 0.1 mg/ml of Rnase. Total DNA was then extracted with phenol-chloroform, ethanol precipitated and dissolved in Tris-EDTA buffer. DNA was electrophoresed in 1.5% agarose gel containing ethidium bromide and visualized under UV light. All the products were purchased from Sigma, exempted proteinase K and RNase (Boehringer Mannheim).

## Apoptose quantification (Hoechst staining)

After a 5 h incubation period in the presence of UA (12, 14, 16 and 18  $\mu$ M), Daudi cells were stained with 0.06  $\mu$ g/ml of the DNA-specific fluorochrome Hoechst 33342 (Sigma) for 10 min. Samples were then washed with PBS, mounted onto glass slides and coverslipped. The morphology of the nuclei was observed and photographed under a fluorescence microscope (Leica) using a 340–380 nm laser line for excitation and 425 nm for detection.

## [Ca<sup>2+</sup>] measurements

Calcium concentration was measured according to the Fura-2/AM technique described by Grynkiewicz *et al.* in 1985.<sup>17</sup> Samples ( $10^6$  cells/ml) were loaded with Fura-2/AM (1  $\mu$ M) in a buffer containing 2% BSA, 110 mM NaCl, 5.4 mM KCl, 25 mM NaHCO<sub>3</sub>, 0.8 mM MgCl<sub>2</sub>, 0.4 mM KH<sub>2</sub>PO<sub>4</sub>, 0.33 mM NaH<sub>2</sub>PO<sub>4</sub>, 20 mM HEPES and 1.2 mM CaCl<sub>2</sub> (pH 7.4). After an incubation period of 45 min at 37°C, cells were washed and resuspended in the same buffer without BSA. [Ca<sup>2+</sup>]<sub>i</sub> was measured by spectrofluorometry (Kontron SFM 25) with monochromator settings of 340 nm (excita-

tion) and 478 nm (emission). Values of  $[Ca^{2+}]_i$  were calculated from the ratio of observed fluorescence intensities ( $F$ ) of the intracellular Fura-2 as follows:

$$[Ca^{2+}]_i = K_d(F - F_{min}) / (F_{max} - F).$$

Maximum and minimum values of fluorescence ( $F_{max}$  and  $F_{min}$ ) were evaluated, respectively, by adding 5  $\mu$ M ionomycin (maximum) and by the following addition of 2 mM  $MnCl_2$  (minimum). A value of 224 nM for the apparent  $K_d$  of binding to Fura-2 at cytoplasmic ionic conditions was applied.<sup>17</sup> With the aim of locating the source of calcium flux, endoplasmic reticulum  $Ca^{2+}$  ATPase inhibitor (thapsigargin 1  $\mu$ M)<sup>18</sup> and voltage-dependent  $Ca^{2+}$  channel blockers (verapamil 1  $\mu$ M,<sup>19</sup>  $\omega$ -conotoxin 1  $\mu$ M,<sup>20</sup>  $LaCl_3$  100  $\mu$ M and  $NiCl_2$  100  $\mu$ M<sup>21</sup>) were employed in some samples. Two sets of experiments were performed: in the presence or absence of external calcium. In this second case,  $Ca^{2+}$ -free medium (medium + 5 mM EGTA) and  $Ca^{2+}$ -free buffer (0 mM  $CaCl_2$  + 1.2 mM EDTA) were employed.

## Results

### Cell viability

The MTT test showed that UA decreases cell viability in Daudi cells in a dose-dependent manner (Figure 1). The estimated  $IC_{50}$  value was 13  $\mu$ M. In ethanol control samples, viability was not

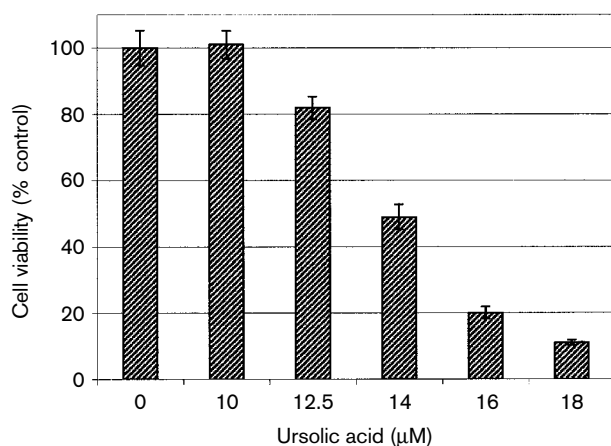


**Figure 1.** UA antiproliferative activity in Daudi cells. Cells were incubated with UA at different concentrations for 24 h. Cell viability was determined by MTT assay as described in Materials and methods. The results were expressed as percentages of the control (untreated cells). Data points represent the mean values of six replicates, with the bars indicating SEM.

affected, even with a maximal ethanol concentration of 0.18%.

### Evaluation of UA cytotoxicity

We monitored the cytotoxic activity of UA on Daudi cells by measuring the LDH activity. The observed effects of UA on cell lysis were time and dose dependent (Figure 2). Nevertheless, the levels of cytotoxicity were relatively low and reached a maximal level of 17% for 18  $\mu$ M UA in a 10 h incubation period.

### Evidence of apoptosis induction by UA

Several tests provided us with evidence that apoptosis was the major phenomenon occurring after UA treatment on Daudi cells:

Firstly, experiments of apoptosis quantification by annexin V/PI staining in flow cytometry gave cytograms showing four populations: living cells (annexin<sup>-</sup> PI<sup>-</sup>), early apoptotic cells (annexin<sup>+</sup> PI<sup>-</sup>), late apoptotic cells (annexin<sup>+</sup> PI<sup>+</sup>), and permeabilized cells (annexin<sup>-</sup> PI<sup>+</sup>). A range of 10–18  $\mu$ M UA and 2, 5, 8 and 24 h incubation times were tested, and we established that the proportion of early apoptotic cells increased on and after 8 h. The cytogram obtained with 18  $\mu$ M UA after an 8 h incubation period is represented in Figure 3. We noticed that the rate of counted early apoptosis cells did not reach 15% whatever the dose and the incubation time. In the

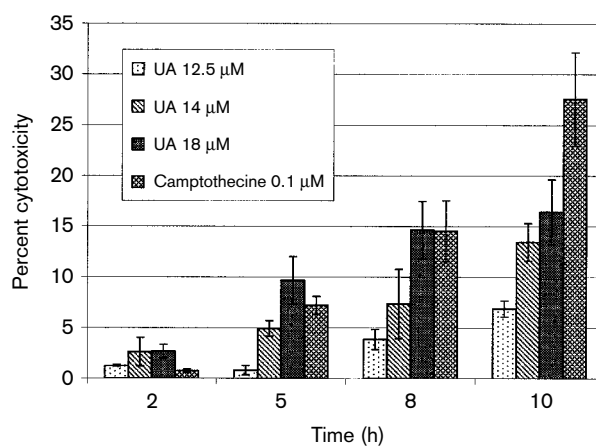


**Figure 2.** Cytotoxic activity of UA in Daudi cells. Cells were treated with different concentration of UA (12.5, 14 and 18  $\mu$ M) for the indicated incubation time. The cytotoxicity percentages were measured by the LDH release assay as described in Materials and methods. Data points represent the mean values of four replicates, with the bars indicating SEM.

same way, the positive apoptosis control camptothecin gave a maximum of 6% of annexin<sup>+</sup> PI<sup>-</sup> cells whatever the conditions (data not shown).

Secondly, genomic DNA was then extracted with a view to obtaining evidence of genomic DNA fragmentation—a hallmark of apoptotic cell death. Several assays were performed, DNA fractions were isolated from UA-treated samples at different incubation times, lysed and subjected to gel electrophoresis. During the first hours of exposure to drug, no DNA laddering was observed in samples treated with UA 14–18  $\mu$ M. With regard to these doses, the first evidence of DNA fragmentation could be observed after a 24 h incubation period. In these conditions, the characteristic internucleosomal pattern of DNA degradation appeared to be dependent on UA concentration, since a dose of 14  $\mu$ M induced no or little DNA fragmentation, whereas 18  $\mu$ M led to a pattern similar to the positive camptothecin control (Figure 4).

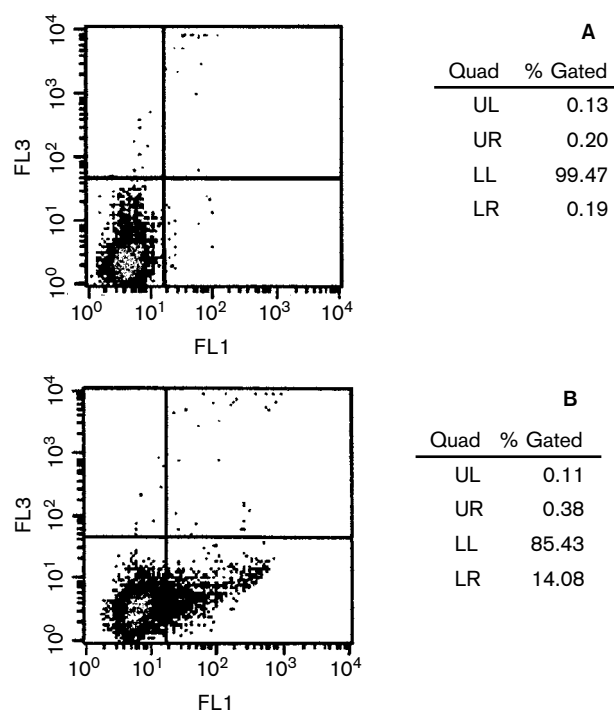


**Figure 3.** Cytofluorograms of annexin V binding (abscissa) versus PI uptake (ordinate). Daudi cells ( $5 \times 10^5$  sample) were stained with annexin V and PI according to the annexin V FLUOS kit instructions (see Materials and methods). (A) Control (untreated cells), (B) Cells incubated with 18  $\mu$ M UA for 8 h. Cells in the lower left region (LL) represent living cells, cells in the lower right region (LR) represent early apoptotic cells, cells in the upper right region (UR) represent late apoptotic cells and cells in the upper left region (UL) represent those with damaged membrane only.

Thirdly, the Hoechst staining method was employed as another quantification technique. This DNA-specific fluorochrome allows rapid and simple identification of condensed nuclei and apoptotic bodies characteristic of apoptotic cells by fluorescence microscopy (Figure 5). In samples treated with different concentrations of UA, these cells could be counted with regard to an untreated control. The

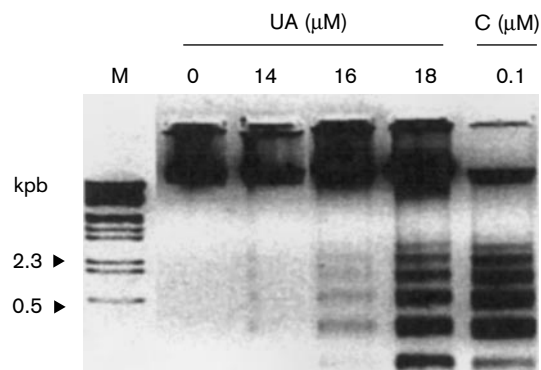


**Figure 4.** Agarose gel electrophoresis of DNA extracted from Daudi cells. Cells were incubated with UA or camptothecin (C) for 24 h. In total,  $10^6$  were collected per assay and total DNA extracted with the phenol–chloroform technique as described in Materials and methods. DNA was electrophoresed on 1.5% agarose gel. The molecular size marker (lane M) was a *Hind*III digest of  $\lambda$  DNA.

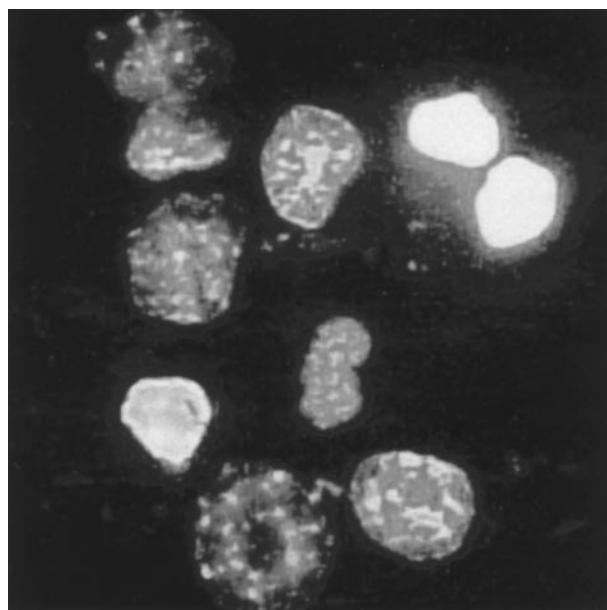


**Figure 5.** Hoechst 33342 staining evaluated morphological alterations of chromatin in Daudi cells. Cells were treated for 5 h with 18  $\mu$ M UA, stained for 10 min with Hoechst 33342 and examined by fluorescence microscopy. Characteristic condensed nuclei of apoptotic cells were brightly stained.

results obtained showed that a percentage of apoptotic cells increased with the concentration of UA in a dose-dependent manner. A maximum of 38% was observed with 18  $\mu\text{M}$  of UA after a 5 h incubation period (Figure 6, curve A).

#### UA-induced calcium mobilization in Daudi cells

Fura-2 is the most useful indicator of intracellular free calcium as it allows precise measurement of low concentrations, around 100 nM, as it is maintained in intracellular media.

Measurement of  $[\text{Ca}^{2+}]_i$  was performed at different times after an exposure to 16  $\mu\text{M}$  UA. Incubation periods of 1, 3, 5 and 7 h did not show any differences compared to the control (data not shown). On the other hand, a 2 h incubation period led to an increase in fluorescence intensity corresponding to a more than 2-fold  $[\text{Ca}^{2+}]_i$  rise ( $324.5 \pm 63$  nM) (Figure 7). Thapsigargin, an ER-calcium ATPase inhibitor,<sup>18</sup> was employed to determine whether this rise was due to calcium release from intracellular stores. Addition of 1  $\mu\text{M}$  thapsigargin stimulated a further rapid  $[\text{Ca}^{2+}]_i$  increase and the  $[\text{Ca}^{2+}]_i$  reached approximately the same concentration obtained after 16  $\mu\text{M}$  UA treatment ( $304 \pm 17$ ) (Table 1). However thapsigargin and 16  $\mu\text{M}$  UA had additive effects on the increases in  $[\text{Ca}^{2+}]_i$ . At this time, the UA-induced calcium flux

appeared to be independent of the intracellular  $\text{Ca}^{2+}$  pool. In addition, experiments performed in calcium-free conditions with 16  $\mu\text{M}$  UA failed to induce increases in  $[\text{Ca}^{2+}]_i$  (Table 1).

Subsequent experiments made use of  $\text{Ca}^{2+}$  channel blockers to explore the mechanism by which UA brings about rises in  $[\text{Ca}^{2+}]_i$ . Lanthanum ( $\text{La}^{3+}$ ) and Nickel ( $\text{Ni}^{2+}$ ) agents, known to block voltage-dependent  $\text{Ca}^{2+}$  channels,<sup>21</sup> completely abolished the effects of UA (Figure 7). Furthermore, verapamil, an organic compound inhibitor of L-type calcium channels,<sup>19</sup> significantly curtailed UA-induced increase in  $[\text{Ca}^{2+}]_i$ . In the same way,  $\omega$ -conotoxin, an inhibitor of N-type calcium channels,<sup>20</sup> significantly lowered the effect of UA on  $[\text{Ca}^{2+}]_i$  (Figure 7). These inhibitors had approximately the same effect.

We chose those least toxic to study the calcium currents influence on UA-induced apoptosis by the Hoechst technique. The apoptosis quantification assay performed using UA samples supplemented with 1  $\mu\text{M}$  verapamil showed a decrease of up to 90% in the number of apoptotic cells counted compared to samples without verapamil (Figure 6, curve B).

## Discussion

UA had a significant antiproliferative effect on various cancer cells (lymphocytic leukemia cells P-388 and L-1210) as well as on human lung carcinoma cells (A549).<sup>2</sup> Similarly, previous studies performed in our laboratory demonstrated that UA reduces *in vitro* the growth of human leukemic HL60, human breast MCF7 and mouse melanoma B16 cells.<sup>8-10</sup> In the present work, we confirmed, on Daudi cells, that UA could be considered a good antiproliferative compound. These human lymphoma B cells seemed to be particularly sensitive to UA even through the  $\text{IC}_{50}$  observed (13  $\mu\text{M}$ ) was quite similar to those observed using other cancer cell lines in our previous studies. The shape of the antiproliferative curve revealed a very strong dose-dependent effect since the surviving fraction at 24 h was reduced from 100 to 10% in [10–18  $\mu\text{M}$ ] (Figure 1).

Cell death did not occur at a specific phase of the cell cycle (data not shown), conversely to the  $\text{G}_1$  cell cycle arrest observed after UA treatment on MCF7 or B16 cells.<sup>9,10</sup> These observations led us to think that the way of action of UA on Daudi cells could be peculiar to this cell type. An evaluation of the necrotic process was performed to estimate the toxicity of UA and the LDH assay showed that a maximum of 17% of cells presented a loss of membrane integrity after 8 h

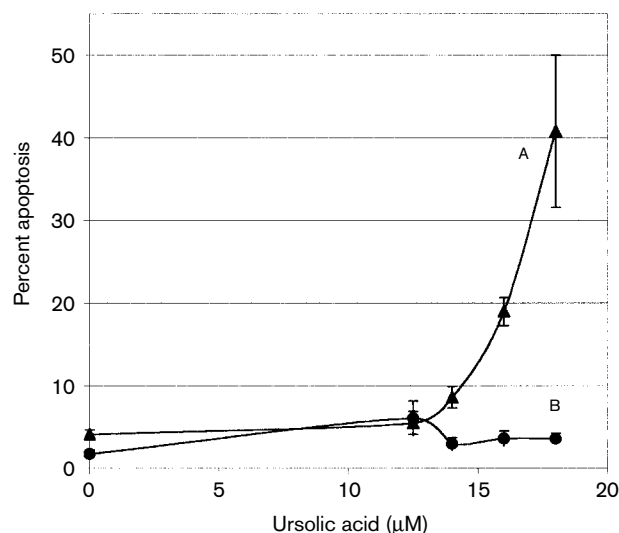


**Figure 6.** Quantification of apoptosis induced by UA in Daudi cells. Cells were incubated with UA at indicated concentrations for 5 h. The percent of apoptotic cells was determined by Hoechst assay as described in Materials and methods. Curve A shows cells treated with UA and curve B shows cells treated with UA + verapamil (1  $\mu\text{M}$ ).

**Table 1.** UA, thapsigargin and calcium-free medium (free  $\text{Ca}^{2+}$ ) effects on intracellular calcium concentration

	Control	UA	Thapsigargin	UA+thapsigargin	Free $\text{Ca}^{2+}$
$[\text{Ca}^{2+}]_i(\text{nM})$	$147.59 \pm 19.75$	$324.5 \pm 63.25$	$304.99 \pm 17.52$	$512.01 \pm 34.62$	$168.11 \pm 21.9$

Thapsigargin (endoplasmic reticulum  $\text{Ca}^{2+}$  ATPase inhibitor) was added at  $1 \mu\text{M}$  15 min before UA treatment of the indicated samples. Daudi cells were incubated for 2 h with UA ( $16 \mu\text{M}$ ) before measurements. Calcium concentration was measured by the Fura-2/AM technique (see Material and methods). Data represent the mean values of four replicates.

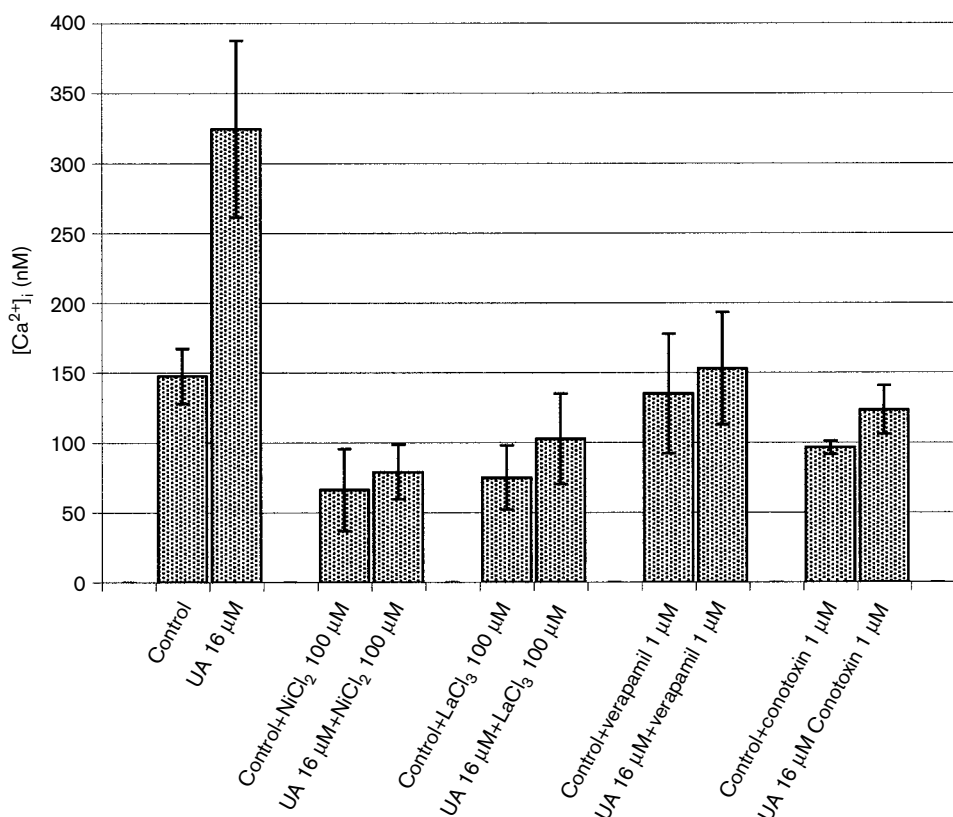


**Figure 7.** Effect of intracellular  $\text{Ca}^{2+}$  inhibitors on UA-induced increased  $[\text{Ca}^{2+}]_i$  in Daudi cells. Cells were incubated with  $16 \mu\text{M}$  UA for 2 h and calcium concentration was measured according to the Fura-2/AM technique (see Materials and methods). Intracellular  $\text{Ca}^{2+}$  inhibitors were added to the cells 15 min before treatment with UA. Data points represent the mean values of four replicates, with the bars indicating SEM.

of treatment (Figure 2). This result indicated that quite a few Daudi cells could be considered necrotic.

With the aim of assessing the part of apoptotic or necrotic cell death, a quantification of these two phenomena was performed using the annexin V/PI technique in flow cytometry. This technique allowed us to distinguish early apoptotic cells from late apoptotic cells or permeabilized cells. These populations were represented on the cytogram (Figure 3) and it was clear that the greater part of the cells were annexin  $\text{V}^+$  first (early apoptotic) before becoming PI loaded (late apoptotic) and that the part of permeabilized cells (only  $\text{PI}^+$ ) considered necrotic was reduced

to a minimum. This adds weight to the fact that there was no UA-induced toxicity on Daudi cells and that the essential way of cell death was apoptosis.

On the other hand, the early apoptosis rate obtained did not attain 15% of the living cells using UA ( $18 \mu\text{M}$  sample, Figure 3) and 6% using camptothecin whatever the incubation time. These low percentages originally seemed to be rather surprising. In fact, such phenomena had already been described on other cell lines and it is usually admitted that early apoptosis is a transitory event, that running time is characteristic of the cell type and that it can be short for some of the latter.<sup>22</sup> This might mean that, in Daudi cells, the 'time

window' through which apoptotic cells were recognized by annexin V-FITC was narrow. This hypothesis led us to consider this staining assay as a good qualitative method, but not a quantitative one, for revealing apoptotic cells in our model.

Conversely, the DNA fragmentation assay performed by gel electrophoresis showed a strong ladder pattern after 24 h of treatment with UA (Figure 4).

Finally, apoptosis quantification was performed by the Hoechst technique and revealed a UA dose-dependent apoptosis rate which reached up to 38% in the 18  $\mu$ M UA sample (Figure 6, curve A). On the other hand, and in the light of previous studies which demonstrated the absolute necessity of calcium for induction of apoptosis,<sup>23-25</sup> we decided to investigate whether this cation was involved in the UA-induced apoptosis observed. Investigations on calcium fluxes monitored with the Fura-2/AM technique showed an increase in fluorescence intensity after incubation with UA. This increase could be achieved by different mechanisms. Firstly,  $\text{Ca}^{2+}$  could be mobilized from intracellular stores such as the mitochondria, nucleus or endoplasmic reticulum.<sup>26</sup> Secondly, the rate of  $\text{Ca}^{2+}$  extrusion from the cytoplasm could be slowed.<sup>27</sup> Finally, plasma membrane channels could open.<sup>28</sup> Our experiments carried out with thapsigargin, an agent known to induce calcium release from the endoplasmic reticulum, showed that the calcium did not proceed from this organite (Table 1). Furthermore, this increase in  $[\text{Ca}^{2+}]_i$  did not occur in 'free calcium' conditions, thus excluding the hypothesis that calcium could come from other intracellular stores. According to the evidence, the calcium came from extracellular medium and could enter into the cell through calcium channels that allow passive movement of  $\text{Ca}^{2+}$  across the membrane. These electrophoretic imports could be divided into three types: L, T and N, where L was the most common type observed.<sup>29</sup> In our experiments, an increase of  $\text{Ca}^{2+}$  after treatment with UA was prevented by preincubation with L- and N-specific voltage channel blockers (verapamil and  $\omega$ -conotoxin), but also by non-specific inhibitors ( $\text{LaCl}_3$  and  $\text{NiCl}_2$ ). So, it seemed that UA-induced this inward calcium current but did not act on a particular type of calcium channel. Therefore it can be excluded that the calcium influxes observed could be due to an unspecific detergent property of the drug.

The action of the calcium blockers used inhibited the calcium influxes but also abolished the UA-induced apoptosis as shown by the Hoechst technique using verapamil (Figure 6, curve B). This provided evidence that apoptosis was mediated by these calcium currents in our cellular model.

The structure of UA (pentacyclic triterpene acid) is very similar to the glucocorticoid hormone. Several studies reported that UA can bind to glucocorticoid receptor and form a complex, resulting in different effects. Among the different effects observed, regulation of the expression of differentiation-specific genes was noticed in F9 teratocarcinoma stem cells and induction of down-regulation of MMP-9 gene in human fibrosarcoma cells.<sup>7,30</sup> On the other hand, Orrenius reported that treatment of immature thymocytes with glucocorticoids induced calcium fluxes. These fluxes were blocked by actinomycin D and cycloheximide, thus showing that gene transcription and protein synthesis were also required in this process.<sup>31</sup> Furthermore, the same effect could be observed in mouse lymphoma cells with a delay of 2 h between the treatment and the intracellular calcium increase, corresponding to the time required to regulate gene transcription.<sup>32</sup>

Our model, i.e. Daudi cells, was reported to be glucocorticoid receptor positive,<sup>33,34</sup> and our results showed that the intracellular calcium increase occurred after 2 h of treatment and triggered biochemical features of apoptosis. Taking into account this information, we hypothesized that UA could bind to the glucocorticoid receptor and that the translocation of this complex could enhance the transcription of genes involved in calcium fluxes, resulting in the increase of cytosolic calcium concentration. The biochemical consequences of calcium elevations resulted in apoptotic cell death via multiple protease activation as has already been described in several models.<sup>35</sup> Nevertheless, we could not totally exclude a second hypothesis according to which UA could integrate with the membrane or bind to another kind of receptor and provoke calcium channels opening via another way. However, UA has not been reported to bind to any other type of receptor except the glucocorticoid one. So, taking account the similarities between our observations and studies described above, we considered that this second hypothesis was quite improbable.

## Conclusion

We showed that UA induced apoptosis in Daudi cells and that this phenomenon was triggered by calcium inward currents. This form of programmed cell death seemed to be a form of glucocorticoid-induced lymphocytolysis, as already described in other models,<sup>35</sup> but in our case calcium seemed to issue exclusively from the extracellular medium. Whether this peculiarity was due to the chemical structure of

UA, which is not a physiological ligand for glucocorticoid receptor, is still unclear. The precise mechanism of formation of the UA-glucocorticoid receptor complex and its biochemical consequences will be the subject of further investigations in our laboratory.

## Acknowledgments

The authors are grateful to Region Limousin and 'Comité Départemental de la Corrèze de la Ligue Contre le Cancer' for their financial assistance.

## References

- Belding RD, Blankenship SM, Young E, Leidy RB. Composition and variability of epicuticular waxes in apple cultivars. *J Am Soc Hort Sci* 1998; **123**: 348-56.
- Lee KH, Lin YM, Wu TS, et al. The cytotoxic principles of *Prunella vulgaris*, *Psychotria serpens*, and *Hyptis capitata*: ursolic acid and related derivatives. *Planta Med* 1988; **54**: 308-11.
- Liu J. Pharmacology of oleanolic acid and ursolic acid. *J Ethnopharmacol* 1995; **49**: 57-68.
- Ohigashi H, Takamura H, Koshimizu K, Tokuda H, Ito Y. Search for possible antitumor promoters by inhibition of 12-O-tetradecanoylphorbol-13-acetate-induced Epstein-Barr virus activation; ursolic acid and oleanolic acid from an anti-inflammatory chinese medicinal plant, *Glechoma Hederaceae* L. *Cancer Lett* 1986; **30**: 143-51.
- Tokuda H, Ohigashi H, Koshimizu K, Ito Y. Inhibitory effects of ursolic acid on skin tumor promotion by 12-O-tetradecanoylphorbol-13-acetate. *Cancer Lett* 1986; **33**: 279-85.
- Huang MT, Ho CT, Wang ZY, et al. Inhibition of skin tumorigenesis by rosemary and its constituents carnosol and ursolic acid. *Cancer Res* 1994; **54**: 701-8.
- Lee H-Y, Chung HY, Kim K-H, Lee J-J, Kim K-W. Induction of differentiation in the cultured F9 teratocarcinoma stem cells by triterpene acids. *J Cancer Res Clin Oncol* 1994; **120**: 513-8.
- Simon A, Najid A, Chulia AJ, Delage C, Rigaud M. Inhibition of lipoxygenase activity and HL60 leukemic cell proliferation by ursolic acid isolated from heather flowers (*Calluna vulgaris*). *Biochim Biophys Acta* 1992; **1125**: 68-72.
- Es-saady D, Simon A, Jayatvignoles C, Chulia AJ, Delage C. MCF7 cell cycle arrest at G<sub>1</sub> through ursolic acid, and increased reduction of tetrazolium salt. *Anticancer Res* 1996; **16**: 481-6.
- Es-saady D, Simon A, Ollier M, Maurizis JC, Chulia AJ, Delage C. Inhibitory effect of ursolic acid on B16 proliferation through cell cycle arrest. *Cancer Lett* 1996; **106**: 193-7.
- Baek JH, Lee YS, Kang CM, et al. Intracellular Ca<sup>2+</sup> release mediates ursolic acid-induced apoptosis in human leukemic HL-60 cells. *Int J Cancer* 1997; **73**: 725-8.
- Wyllie AH, Kerr JFR, Currie AR. Cell death: the significance of apoptosis. *Int Rev Cytol* 1980; **68**: 251-306.
- Arends MJ, Morris RG, Wyllie AH. Apoptosis, the role of the endonuclease. *Am J Pathol* 1990; **136**: 593-608.
- Miyashita Y, Reed JC. Bcl2 oncoprotein blocks chemotherapy-induced apoptosis in a human leukemia cell line. *Blood* 1993; **81**: 151-7.
- Johnson N, Ng TT, Parkin JM. Camptothecin causes cell cycle perturbations within T-lymphoblastoid cell followed by dose dependent induction of apoptosis. *Leuk Res* 1997; **21**: 961-72.
- Mosman T. Rapid colorimetric assay for cellular growth and survival: application to proliferation and cytotoxicity assays. *J Immunol Methods* 1983; **65**: 55-63.
- Gryniewicz G, Poenie M, Tsien RY. A new generation of Ca<sup>2+</sup> indicators with greatly improved fluorescence properties. *J Biol Chem* 1985; **260**: 3440-50.
- Thastrup O, Cullen PJ, Dobrak BK, Hanley MR, Dawson AP. Thapsigargin, a tumor promoter, discharges intracellular Ca<sup>2+</sup> stores by specific inhibition of the endoplasmic Ca<sup>2+</sup>-ATPase. *Proc Natl Acad Sci* 1990; **87**: 2466-70.
- Fleckenstein A. Specific pharmacology of calcium in myocardium, cardiac pacemakers, and vascular smooth muscle. *Annu Rev Pharmacol Toxicol* 1977; **17**: 149-66.
- Olivera BM, McIntosh J, Zeikus R, et al. Peptide neurotoxins from fish-hunting cone snails. *Science* 1985; **230**: 1338-43.
- Tsien RY. Intracellular measurements of ion activities. *Annu Rev Biophys Bioeng* 1983; **12**: 91-116.
- Del Bino G, Darzynkiewicz Z, Degraef C, Mosselmanns R, Fokan D, Galand P. Comparison of methods based on annexinV binding, DNA content or TUNEL for evaluation cell death in HL60 and adherent MCF7 cells. *Cell Prolif* 1999; **32**: 25-37.
- Hameed A, Olsen KJ, Lee MK, Lichtenheld MG, Podak ER. Cytolysis by Ca<sup>2+</sup>-permeable transmembrane channels: pore formation causes extensive DNA degradation and cell lysis. *J Exp Med* 1989; **169**: 765-77.
- McConkey DJ, Hartzell P, Perez JF, Orrenius S, Jondal M. Calcium-dependent killing of immature thymocytes by stimulation via the CD3/T cell receptor. *J Immunol* 1989; **143**: 1801-6.
- Odaka C, Kizaki H, Tadakuma T. T cell receptor-mediated DNA fragmentation and cell death in T cell hybridomas. *J Immunol* 1975; **144**: 2096-101.
- Hesketh TR, Moore JP, Morris JDH, Taylor JR, Smith GA, Metcalfe JC. A common sequence of calcium and pH signals in the mitogenic stimulation of eukaryotic cells. *Nature* 1985; **313**: 481-4.
- Tolloczko B, Jia YL, Martin JG. Serotonin-evoked calcium transients in airway smooth muscle cells. *Am J Physiol* 1995; **269**: 234-40.
- Hagiwara S. Calcium channel. *Annu Rev Neurosci* 1981; **4**: 69-125.
- Carafoli E. Intracellular calcium homeostasis. *Annu Rev Biochem* 1987; **56**: 395-433.
- Cha HJ, Park MT, Chung HY, et al. Ursolic acid-induced downregulation of MMP9 gene is mediated through the nuclear translocation of glucocorticoid receptor in HT1080 human fibrocarcinosoma cells. *Oncogene* 1998; **16**: 771-8.
- McConkey DJ, Nicotera P, Hartzell P, Bellomo G, Wyllie AH, Orrenius S. Glucocorticoids activate a suicide process in thymocytes through an elevation of cytosolic Ca<sup>2+</sup> concentration. *Arch Biochem Biophys* 1989; **269**: 365-70.



32. Lam M, Dubyak G, Distelhorst CW. Effect of glucocorticoid treatment on intracellular calcium homeostasis in mouse lymphoma cells. *Mol Endocrinol* 1993; **7**: 686-93.
33. Elliot KRF, Princler GL, Urba WJ, Faltynek CR. Synergistic antiproliferative effects of glucocorticoids and interferon-A on some lymphoid cell lines. *J Cell Physiol* 1988; **134**: 85-92.
34. Dietrich JB, Chasserot-Golaz S, Beck G, Bauer G. Antagonism of glucocorticoid induction of Epstein-Barr virus early antigens by different steroids in Daudi lymphoma cells. *J Steroid Biochem* 1986; **24**: 417-421.
35. McConkey D, Orrenius S. The role of calcium in the regulation of apoptosis. *Biochem Biophys Res Commun* 1997; **239**: 357-66.

*(Received 22 July 2000; accepted 1 August 2000)*